DYNAMICS OF SPAN MORPHING HELICOPTER ROTOR

Deepika Vangeti, Dr. M. Senthil Murugan
Aero-Electro-Mechanics & Systems (AIMS) Lab
Department of Aerospace Engineering,
Indian Institute of Technology Madras
Chennai, India 600036
Email: drsen@iitm.ac.in

Abstract:

Variable span morphing rotor blade can vary its radius during the flight and can improve the flight performance and flight dynamics significantly. In this study, the dynamics of a span morphing rotor blade is modeled and analysed. A telescopic-box beam type mechanism is considered for realizing the span morphing blade. The telescopic wing had two beams, a primary beam attached to the rotor hub and a secondary beam that can morph along radial direction. The dynamics induced by span morphing is captured as moving loads over the primary beam. The morphing dynamic equations are derived using the approximate energy methods. The effect of key morphing parameters such as span morphing speed, magnitude of morphing loads and rotor speed on the flap dynamic response of primary beam are studied. Results show that the speed of span morphing has significant impact on the flap dynamic response. Also, the magnitudes of span morphing loads have considerable impact. In contrast, rotor speed during span morphing has inverse effects on the flap response because of the coupled effect of loss of centrifugal stiffness and addition of morphing induced dynamic loads. Therefore, in general, the morphing induced dynamics plays a significant role in the design of span morphing rotor.

1.INTRODUCTION:

Helicopters rotor blades play a crucial role in control and performance related challenges of the whole helicopter. Conventional rotor blades are typically designed for particular flight condition and therefore not optimal at other flight conditions[1].

Morphing structures or wings can be used to design the wings that can change its geometry, on flight, such that it is optimal at each flight condition. These wing morphing methodologies include the in plane planform alteration (includes sweep, span and chord changes), out of plane alteration (includes twist, dihedral/gull and span wise bending), airfoil adjustment (includes camber, thickness changes) [2].

Studies have shown that morphing wing can increase the payload, fuel efficiency, range, maximum speed and altitude, and also reduce the vibrations and noise more efficiently when compared to rotor blades with a fixed geometry [2].

Variable wing or span morphing is a promising technology allows the large scale changes in wing aspect ratio which provide the optimal rotor radius for various helicopter flight conditions [3] [4].

Fradenburgh *et al.*[5] investigated the span morphing wing concept for a tilt rotor. Lower diameter rotor during cruise resulted in lower tip speeds and high disc loading that significantly improved the efficiency of fuel consumption. Higher diameter in hovering results in lower disc loading and reduced the power requirement by 30%. Gandhi *et al*.[6] did the performance analysis of different morphing concepts for a dynamic rotor blade shape.

Many of the span morphing studies mainly focused on performance analysis and only few studies have focused on aeroelasticity of span morphing wing. Jae sung Bae *et al*.[3] studied the static and dynamic aeroelastic response of the span morphing cruise missile. Wing was modelled as a box wing structure which has one fixed wing box and other movable wing box that extends from the main wing box. A subsonic doublet hybrid method (DHM) was used for the computation of the subsonic aerodynamic forces. The aeroelastic analysis shown that variable span morphing wing requires more bending stiffness than the torsional stiffness.

Murugan *et al*.[7] studied the aeroelastic response and stability of span morphing, fixed wing aircraft. They modelled the span morphing wing as a telescopic beam and aeroelastic simulations were performed with thin airfoil theory and the span morphing induced aerodynamic effects. Results have shown a significant reduction in flutter velocity during span morphing dynamic process. Denil *et al* [8]. investigated the dynamics of span morphing wing where they modelled wing as axially moving telescopic beam. The morphing part of beam is modelled as moving loads over a host beam. The dynamic response is amplified and shown unconventional response behaviour.

Only few studies have focused on span morphing rotor blades and they are also focused on the performance analysis. It is necessary to study the modelling and dynamics of the span morphing rotor during the morphing and after morphing process. Therefore, this study focuses on the dynamic analysis of span morphing helicopter rotor by modelling it as moving load problem. The dynamic equations are solved using approximate methods and the numerical results are analysed for various cases of span morphing process.

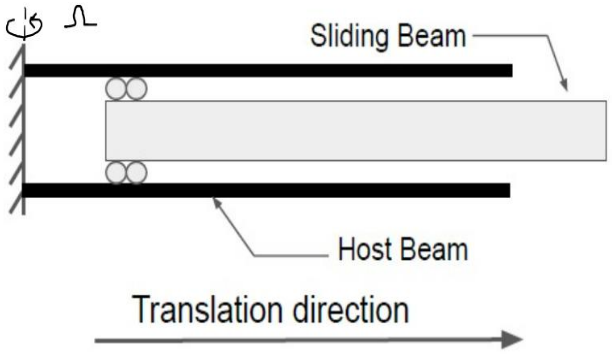

Fig:1 Schematics of Span morphing rotor blade

2. DYNAMICS OF MORPHING ROTATING BLADE

2.1 Dynamic Model of Rotating Blade

Generally, the rotor blades are modeled as rotating beam with flap, lag and torsion motions. The flapping response plays the primary role in the dynamics and aeroelasticity of rotor. Therefore, in this study, only the flapping response is considered. The equation of motion (EoM) for flapping motion based on Euler-Bernoulli beam theory can be given as

$$(1) \qquad \frac{\partial^2}{\partial x^2}\left(EI\,\frac{\partial^2 w}{\partial x^2}\right) + m\,\frac{\partial^2 w}{\partial t^2} - \frac{m\Omega^2 R^2}{2}\frac{\partial}{\partial x}\left[\left(1-\frac{x^2}{R^2}\right)\frac{\partial w}{\partial x}\right] = F(x,t)$$

Here, the blade parameters in the equation are given as: EI = flap bending stiffness, w = flap deflection,
m = mass per unit length, R = blade radius,
Ω = rotational speed, and $F(x,t)$ = external force per unit length.

2.2 Dynamic Formulation of Span Morphing Rotor Blade

In this section, dynamic model of rotor blade undergoing the span morphing is modeled. The morphing blade is modeled as a telescopic type beam. That is the blade has a two beams:
a) A primary host beam attached to the rotor hub.
b) A secondary beam that can protrude outside or retract inside the primary host beam.
In this study, the secondary beam is modeled as the moving loads over the primary host beam as shown Fig.1.

The moving loads induced by morphing-secondary beam typically include the moving force and moving moment. These moving loads are included in the energy formulation using the Dirac-delta function. The moving force is assumed to have magnitude "$\boldsymbol{f_0}$" and moving with velocity "$\boldsymbol{c_1}$". Similarly, amplitude of moving moment is "$\boldsymbol{M_0}$" and moving with a morphing velocity"$\boldsymbol{c_2}$". However, for the morphing beam study, the velocity $\boldsymbol{c_1}$ and $\boldsymbol{c_2}$ can be considered to be equal.

For the preliminary results, the flapping equation of motion (EoM) for the host blade is derived based on the energy methods. Rayleigh-ritz approach with Lagrange's equation is used to develop the equations of motion. Rayleigh-ritz method typically assumes the modes shapes that satisfy the geometrical boundary conditions. In this study, the flapping displacement is assumed to be

$$\boldsymbol{w_{(x,t)}} = \sum_{i=1}^{N} \boldsymbol{\gamma_i(x) q_i(t)}$$

Rotor blade is modelled as a cantilever beam whose geometric boundary conditions are

$$w_{(x,t)} = 0\,;at\ x = 0$$

$$\frac{dw}{dx} = 0\,; at\ x = 0$$

Therefore, the admissible approximate function, $\gamma_i(x)$ must satisfy geometric boundary conditions, i.e

$$\gamma_i(0) = 0;\ \frac{d\gamma_i(0)}{dx} = 0\,;$$

In this study, for initial results, a polynomial shape function is assumed as

$$\boldsymbol{w}_{(\boldsymbol{x},\boldsymbol{t})} = \sum_{\boldsymbol{i=1}}^{\boldsymbol{N}} \frac{x^{i+1}}{R^{i+1}} \boldsymbol{q_i(t)}$$

Once, the approximate functions are assumed, the kinetic and potential energies, and work done by the moving loads can be calculated as given below.

$$\text{Kinetic energy } T = \int_0^R \frac{1}{2} m \left(\frac{\partial w}{\partial t}\right)^2 dx$$

$$= \int_0^R \frac{1}{2} m \left(\sum_{i=1}^{N} \gamma_i(x)\dot{q}_i\right)\left(\sum_{j=1}^{N} \gamma_j(x)\dot{q}_j\right) dx$$

$$= \frac{1}{2}\sum_{i=1}^{N}\sum_{j=1}^{N} m_{ij}\dot{q}_i\dot{q}_j$$

where,

$$m_{ij} = \int_0^R m\gamma_i\gamma_j\, dx$$

Similarly, the potential energy for rotating blade is given as

$$Strain\ energy(\pi) = SE_{flexure} + SE_{cenrifugal\ force}$$

$$= \int_0^R \frac{1}{2} EI \left(\frac{\partial^2 w}{\partial x^2}\right)^2 dx + \int_0^R \frac{1}{2} p(x) \left(\frac{\partial w}{\partial x}\right)^2 dx$$

$$= \int_0^R \frac{1}{2} EI\left(\sum_{i=1}^{N} \gamma_i{}'' q_i\right)\left(\sum_{j=1}^{N} \gamma_j{}'' q_j\right) dx +$$

$$\int_0^R \frac{1}{2} p(x) \left(\sum_{i=1}^{N} \gamma_i{}' q_i\right)\left(\sum_{j=1}^{N} \gamma_j{}' q_j\right) dx$$

$$= \frac{1}{2}\sum_{i=1}^{N}\sum_{j=1}^{N} k_{ij} q_i q_j$$

Where,

$$k_{ij} = \int_0^R EI\gamma_i{}''\gamma_j{}''\, dx + \int_0^R p(x)\,\gamma_i{}'\gamma_j{}' dx$$

Centrifugal force, $p(x) = \int_x^R m\Omega^2 x\, dx$

$$= \frac{mR^2\Omega^2}{2}\left(1 - \frac{x^2}{R^2}\right)$$

Now the virtual work done due to moving induced loads can be given by

$$\delta W = \int_0^R f(x,t)\delta(x - c_i t)\delta w dx$$

$$= \sum_{i=1}^{N} Q_i\, \delta q_i$$

Where,

$$Q_i = \int_0^R f\, \delta(x - c_i t)\gamma_i\, dx$$

Now, using Euler-Lagrangian equation:

$$\boldsymbol{\frac{\partial}{\partial t}\left(\frac{\partial T}{\partial \dot{q}_i}\right) - \left(\frac{\partial T}{\partial q_i}\right) + \left(\frac{\partial \pi}{\partial q_i}\right)} = Q_i$$

for $i = 1,2, \ldots. N$

$$\sum_{j=1}^{N} (m_{ij}\, \ddot{q}_j + k_{ij} q_j) = Q_i \quad i = 1,2, \ldots. N$$

These are N coupled equations that can be put together in matrix form

$$\tilde{m}_{ij}\ddot{q}_j + \tilde{k}_{ij} q_j = \tilde{Q}_i \quad i = 1,2, \ldots. N$$

Now, for the moving loads problem, the virtual work is due to the moving force and moving moments induced by morphing secondary beam. Therefore, the virtual work done by moving force and moving moment is given below as two cases. The polynomial shape function of order N=1 and N=3are considered in this study for deriving the equations of motion. The shape function of order 1 is assumed to develop an approximate single degree of freedom that gives approximate analytical solutions of the dynamic response.

Case a: Moving force dynamics

For the assumed mode shape of order one (N=1),

$$\delta W = \int_0^R f_0 \delta(x - c_1 t) \frac{x^2}{R^2} \delta q \, dx$$

And the generalized force is

$$Q = \int_0^R f_0 \delta(x - c_1 t) \frac{x^2}{R^2} \, dx$$

$$Q = f_0 \frac{{c_1}^2 t^2}{R^2}$$

However, the moving load induces two conditions of dynamics in the time domain. That is, the first stage of dynamics during the morphing process or when the force is still moving in the primary beam. In the second stage, the moving load stops at the end of the primary beam but induces dynamic effects for further time period. Therefore, the two equations of motion for the span morphing rotating blade under moving force can be given as,

For stage 1, when $t < S1$

(2) $$\boldsymbol{Q} = \boldsymbol{f_0} \frac{\boldsymbol{{c_1}^2 t^2}}{\boldsymbol{R^2}}$$

For stage 2, when $t > S1$

(3) $$\boldsymbol{Q} = \boldsymbol{f_0} \frac{\boldsymbol{SP^2}}{\boldsymbol{R^2}}$$

$$q(S1) = \alpha_{1m} \; ; \dot{q}(S1) = \beta_{1m} \; ;$$

Here, the initial conditions $q(S1)$ and $\dot{q}(S1)$ are the values at the time **"S1"** when the morphing process has ended at "R=SP".

Case b. Moving moment dynamics

Now, the moving moment can be modeled as

$$M = M_0 \delta(x - c_2 t)$$

Here, the moment is moving at an amplitude M_0 and velocity 'c_2'. The kinetic and strain energy remains the same as moving force case whereas the work done due to moving moment is done as

$$W = \int_0^R M_0 \delta(x - c_2 t) \left(\frac{\partial w}{\partial x}\right) dx$$

And the generalized force, for N=1, is given as

(4) $$\boldsymbol{Q} = \frac{\boldsymbol{2M_0 c_2 t}}{\boldsymbol{R^2}}$$

Case c: Moving force dynamics

Similar to the case of N=1, now considering N=3, or three modes satisfying the boundary conditions, the assumed displacement can be given as,

$$\boldsymbol{w_{(x,t)}} = \sum_{\boldsymbol{i=1}}^{\boldsymbol{N}} \frac{x^{i+1}}{R^{i+1}} \boldsymbol{q_i(t)}$$

The corresponding equations of motion are derived and given as follows.

Equation of motion can be expressed as

(5) $$\boldsymbol{M\ddot{q}} + \boldsymbol{Kq} = \boldsymbol{f}$$

where,

$$\boldsymbol{f} = f_0 \begin{bmatrix} \frac{{c_1}^2 t^2}{R^2} \\ \frac{{c_1}^3 t^3}{R^3} \\ \frac{{c_1}^4 t^4}{R^4} \end{bmatrix}$$

The M, K in the equation of motion corresponds to the matrices of rotating beam.

Case d: Moving moment dynamics

Similarly, the equation of motion for moving moment for N =3 can be expressed as,

(6) $$\boldsymbol{M\ddot{q}} + \boldsymbol{Kq} = \boldsymbol{f}$$

$$\boldsymbol{f} = M_0 \begin{bmatrix} \frac{2c_2 t}{R^2} \\ \frac{3{c_2}^2 t^2}{R^3} \\ \frac{4{c_2}^3 t^3}{R^4} \end{bmatrix}$$

3. NUMERICAL RESULTS:

In this section, the numerical simulations are performed with the Bo105 hingeless rotor blade properties given in Table [1]. These structural properties are considered for the rotating primary beam.

The key variables that affect the dynamics of rotating primary beam or rotor are
a) Rotating speed
b) Speed of the moving loads, i.e.,deployment of secondary beam c_i
c) Magnitude of moving loads induced by the secondary morphing beam.
Therefore, the effects of these variables on the dynamics of rotating blade with moving loads are studied

	Properties	Values
1	Radius, R (m)	4.94
2	Hover tip speed, (m/s)	198.12
3	Mass per unit length, m (kg/m)	6.46
4	Flap, EI z(N-m^2)	1.4340e+5

Table 1. Bo105 rotor properties (Ref.9)

The dynamic response of flapping motion, of primary rotating beam, is studied as two cases of the moving load and moving moments. Also, as mentioned in theory section above, the time domain is divided into two regions:

1) Initial stage in which the morphing is in process or the loads are moving from the fixed end to free end
2) Second stage, in which the morphing process is completed or the moving loads ceased at the tip of the primary beam.

These cases are discussed in the following sections.

3.1 Flap Dynamics and Moving Force

Here, the dynamic tip response of the primary beam due to moving force is discussed

Stage 1: Flap response during morphing

Initially, the flap response during span morphing is evaluated for one revolution and shown in Fig. 2, Fig 3, and Fig. 4

The dynamic responses with respect to the different morphing velocities (5-100m/s) are plotted in Fig:3. The result shows the amplitude of response significantly increases with the morphing speed. Also, there is significant oscillation at higher morphing speeds even during the initial revolution of rotor. This is because the morphing induced forces increases with span morphing speeds as seen from EoM.

Similarly, the effect of rotating speed on the morphing dynamics is studied and shown in Fig 4. The results show that the morphing induced response increases with the decrease in rotating speed. This is because the rotating speed is adding centrifugal stiffness into the system.

Stage 2: Flap response after morphing

Now, the flap response of the primary rotating beam after the moving force reaches the tip is simulated. That is, the time domain response after the morphing process is stopped. The flap responses for two revolutions with various morphing speeds are shown in Fig 5, and 6. Similarly, the responses for various RPMs are given 7.

Fig :5 shows that for a lower span morphing speed (5m/s), the magnitude of flap tip response is lesser for first revolution but the response increases in the subsequent revolutions. Thus lower morphing speeds can result in higher tip deflections of rotor blade in the later revolutions. However, for higher morphing speed, the response reaches its maximum almost during the first revolution. Interestingly, the mean of oscillation remains the same but only there is a phase change. The mean of oscillation mainly depends on the magnitude of the moving load rather than its moving speed. And the phase depends on the moving speed. However, this difference is less when the moving speeds are of closer values as shown in Fig. 6

Fig:7 shows the flap response for different rotor speeds, with the force moving at same speed. The flap response shows two peak oscillations on the second revolution of rotor for lower RPM. However, it shows a single peak with lesser amplitude for the higher RPM. In other words, the oscillation frequency and amplitude of blade response simultaneously increases for the morphing at the lower RPM.

Fig 8 shows the variation of tip response with respect to the magnitude of moving force. It shows the amplitude of tip response is directly proportional to the magnitude of moving force however the impact is less campared to the variation in rotor or moving speeds.

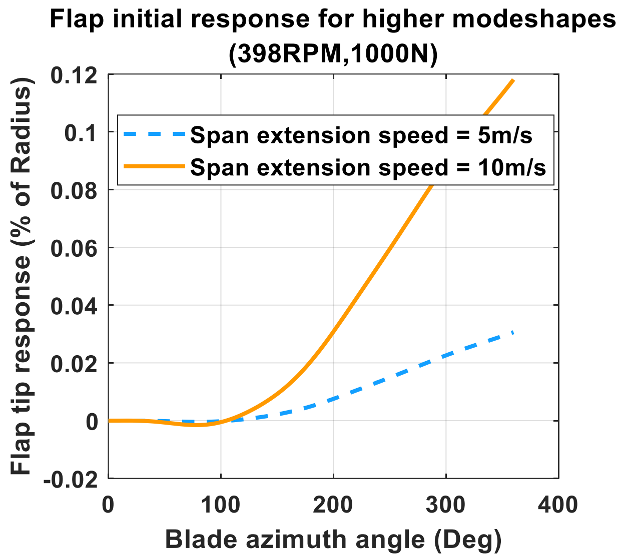

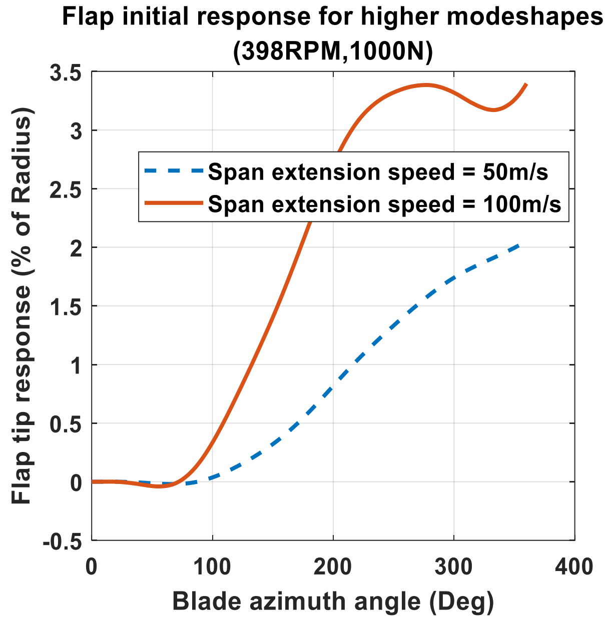

Fig : 2 Flap response at lower morphing speeds

Fig : 3 Flap response at higher morphing speeds

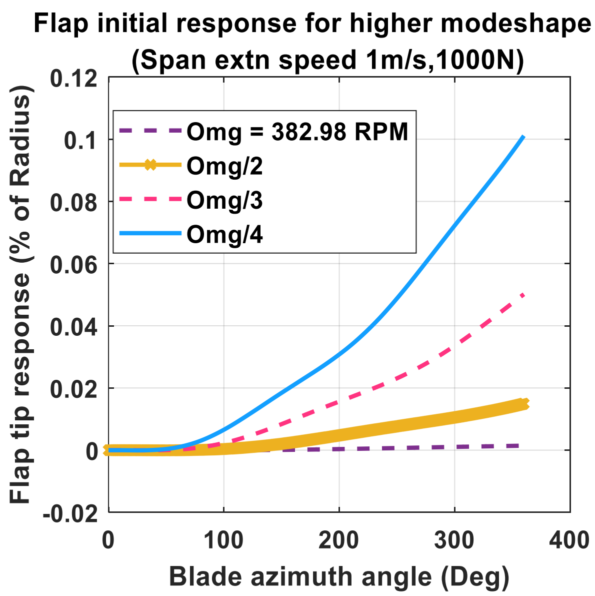

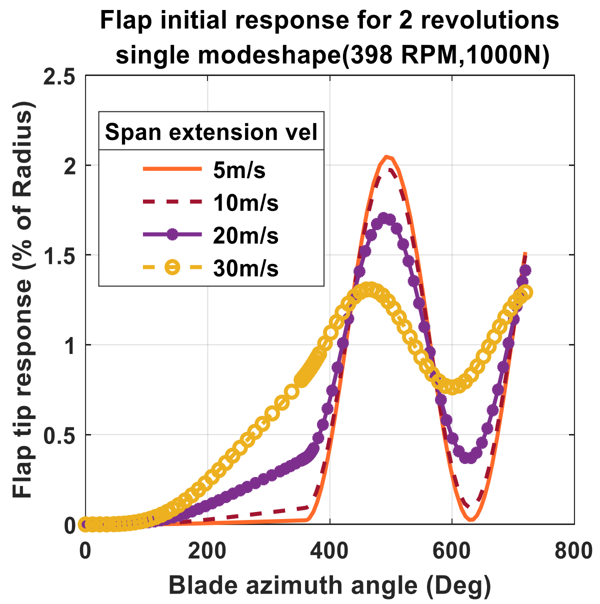

Fig : 4 Flap response vs morphing rotor speeds

Fig : 5 Flap response vs span morphing speeds

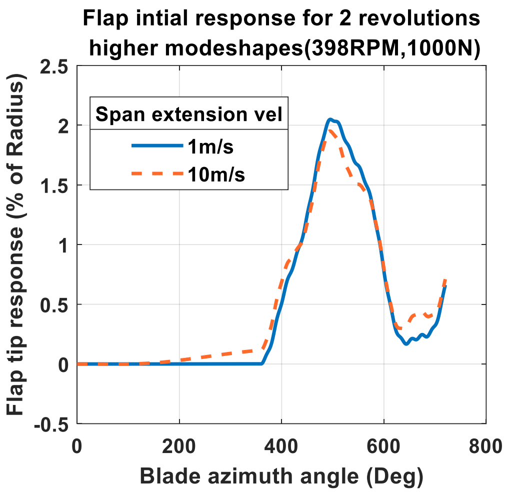

Fig : 6 Flap response vs span morphing speeds

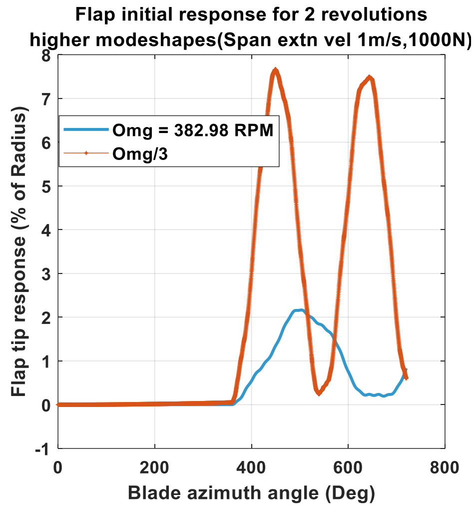

Fig : 7 Flap response vs span morphing rotor speeds

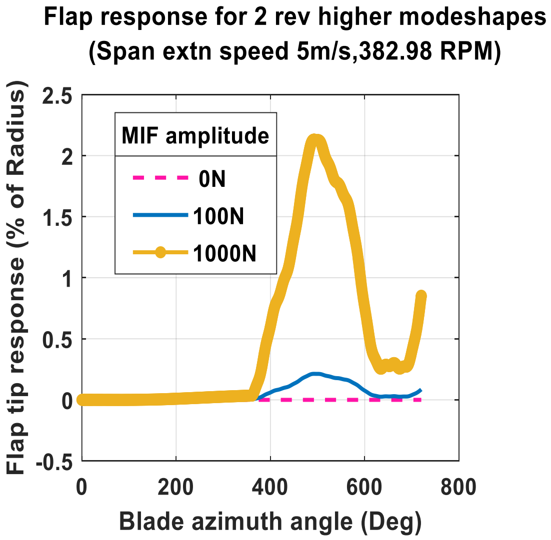

Fig : 8 Flap response vs Morphing induced force(MIF) amplitude

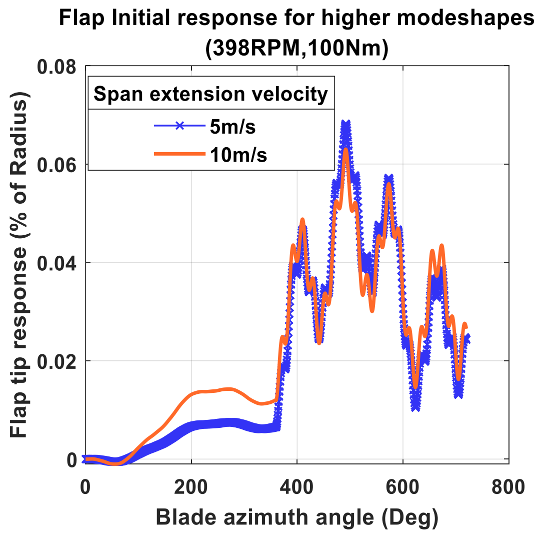

Fig : 9 Flap response vs span morphing speeds

3.2 Flap Dynamics and Moving Moment

Here, the dynamic tip response of the primary beam due to moving moment induced by span morphing is discussed. Flap response is evaluated for morphing induced moment of amplitude M_0 moving with a speed of c_2 as discussed in section 3.1b. Unlike, the moving force results, here the results are shown for 2 revolutions that include both during the morphing and post morphing response. The variations are evaluated for 2 rev under varying morphing velocity and varying rotor speed as shown in figures 9 and 10 respectively.

As the morphing speed c_2 is increased, the flap tip response is also increasing but not monotonically as observed in case of Morphing induced force. For higher speeds, the increase in flap tip response is significant initially but lesser than lower speed amplitude in subsequent revolution. The moving moment induce significant harmonics in the flap response as shown in Fig:9.

Fig 10 shows the flap response with the various rotor speed. Similar to the moving force, the lesser rotor speed induces large amplitude oscillations and increase in number of frequency.

4. CONCLUSION

Dynamic modelling and analysis of span morphing helicopter rotor is performed in this study. A telescopic box beam type mechanism is used to model the span morphing rotor. The span morphing induced dynamic effects on the primary rotating blade are captured via the dynamics of moving force and moving moment. The dynamic simulations are performed with approximate methods. Numerical simulations are performed for various morphing conditions and the following conclusions are drawn:

I. Modelling of Span Morphing Wing: Modelling the span morphing rotor with a telescopic box beam type mechanism allows the physical realization of morphing rotor with less complexity and also an efficient way to theoretical modeling and analysis of morphing process.

II. The effect of the moving speed of loads, magnitude of moving loads, and rotor speed on the dynamic response of flap motion is evaluated. The results for moving force and moving moments are discussed separately.

1) **Dynamics of moving force**:
The results for flap response due to moving force are given below.

a) **Effects of morphing Speed:** The result shows the amplitude of response significantly increases with the morphing speed. There is significant oscillation at higher morphing speeds even during the initial revolution of rotor. This is because the morphing induced forces are quadratically proportional to the span morphing speed as shown in the equations.

For a lower morphing speed (5m/s), the amplitude of flap tip response is lesser for the initial revolution but the response increases in the subsequent rotor revolutions. Thus span morphing with a lower speed can result in higher tip deflections of rotor blade in the later revolutions. For higher morphing speed, the response reaches its maximum almost during the first rotor revolution.

b) **Effects of rotor speed:** The flap response due to span morphing induced dynamics increases with the decrease in rotating speed. This is because the coupled effect of loss of centrifugal stiffness and the additional moving loads. In general, the mean of flap response oscillations mainly depends on the magnitude of the moving load rather than its moving speed. However, the peak amplitude and the phase mainly depend on the moving speed.

c) **Effects of moving loads amplitude:** Results show that the amplitude of flap response is directly proportional to the magnitude of moving loads. However, the impact is less compared to the variation in rotor speed or moving load speeds.

2) **Dynamics of moving moment**:
The flap tip response increases with moving moments speed. However, the increase in flap response is not monotonic as observed in case of morphing induced force. Also, the moving moment induces significant harmonics in the flap response. The other effects of moving moment are similar to that of moving force.

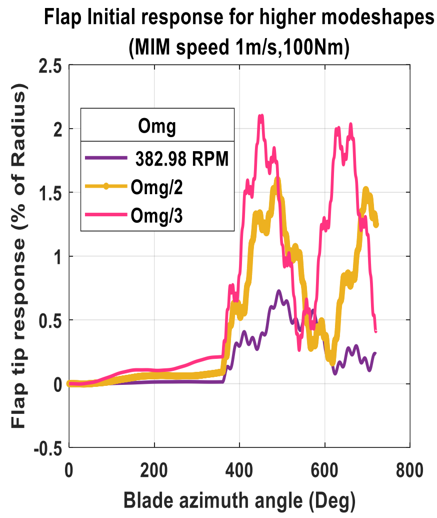

Fig : 10 Flap response vs span morphing rotor speeds

5. REFERENCES

[1] Dr. G. Jorden Leishman, Principles of Helicopter aerodynamics, cambridge,UK: THE PRESS SYNDICATE OF UNIVERSITY OF CAMBRIDGE, 2000.

[2] S.Barbarino, O. Bilgen, R. M. Ajaj, M. I. Friswell,D. J. Inman "A review of morphing aircraft," *Journal of Intelligent Material Systems and Structures,* pp. 823-877, 22 (9) (2011).

[3] Jae-Sung Bae, T. Michael Seigler, and Daniel J. Inman "Aerodynamic and Static Aeroelastic Charecteristics of a Variable-Span Morphing Wing," *Journal Of Aircraft,* vol. 42, no. No.2, March-April 2005.

[4] Brender, S., Mark, H. and Aguilera, F "The Attributes of a Variable-Diameter Rotor System Applied to Civil Tiltrotor Aircraft," NASA Contractor Report,Ames Research Center, NASA-CR-203092, 1997

[5] Fradenburgh, E. and Matuska,D "Advancing Tiltrotor State-of-the-Art with Variable Diameter Rotors," in *Proceeedings of American Helicopter Society 48th Annual Forum*, Washington,DC, 1992

[6] Hao Kang , Hossein Saberi, Farhan Gandhi, "Dynamic Blade Shape for Improved Helicopter Rotor performance," *Journal of American Helicopter society,* vol. 55, no. 032008, 2010.

[7] Senthil Murugan, James H.S.Fincham,M.I.Friswell,D. J. Inman "Aeroelastic Modelling of Morphing Aircraft Wings," in *4th Aircraft Structural Design Conference*, Belfast,UK, 2014.

[8] Denil Chawda, Senthil Murugan "Dynamic Response of a Cantileverd beam Under Combined Moving Moment,Torque and Force," *International Journal of Structural Stability and Dynamics,* 2050065, p. 30, 2020

[9] Senthil Murugan, M., Ganguli, R. and Harursampath, D., " Stochastic Aeroelastic Analysis of Composite Helicoptr Rotor," *J. Am. Helicopter Soc.*, 56(1), 2011.